Single-Molecule Studies

International Edition: DOI: 10.1002/anie.201708705
German Edition: DOI: 10.1002/ange.201708705

Single-Molecule Monitoring of the Structural Switching Dynamics of Nucleic Acids through Controlling Fluorescence Blinking

Kiyohiko Kawai, Takafumi Miyata, Naohiko Shimada, Syoji Ito, Hiroshi Miyasaka, and Atsushi Maruyama**

Abstract: *Single-molecule fluorescence resonance energy transfer (smFRET) is a powerful tool to investigate the dynamics of biomolecular events in real time. However, it requires two fluorophores and can be applied only to dynamics that accompany large changes in distance between the molecules. Herein, we introduce a method for kinetic analysis based on control of fluorescence blinking (KACB), a general approach to investigate the dynamics of biomolecules by using a single fluorophore. By controlling the kinetics of the redox reaction the blinking kinetics or pattern can be controlled to be affected by microenvironmental changes around a fluorophore (rKACB), thereby enabling real-time single-molecule measurement of the structure-changing dynamics of nucleic acids.*

Advances in single-molecule fluorescence microscopy in the last two decades have allowed us to reveal many important biochemical and cellular processes.[1–5] Single-molecule fluorescence measurement is especially effective for investigating the dynamic reaction and motion of biomolecules.[6–10] One of the most successful approaches is the observation of fluorescence resonance energy transfer between a single pair of fluorophores (smFRET).[11–14] The dynamics of distance changes between two sites on biomolecules or between two different molecules can be measured by monitoring time-dependent fluctuation in the donor and acceptor fluorescence signals. This information is usually inaccessible in ensemble measurements due to a lack of synchronization of dynamic motions or of the reactions of biomolecules. While smFRET is a powerful tool and offers fruitful information on various dynamic reactions and the motions of biomolecules, it nevertheless has two disadvantages. One is that it can be applied only to dynamics that accompany large distance changes between two fluorophores (>2 nm). The other is the need to label biomolecules with two fluorophores. Thus the development of a method that requires the labeling of only a single fluorophore to provide dynamic information on biomolecules is highly desired.

To date, chemists have developed various environment-sensitive fluorophores.[15–20] These fluorophores undergo fluorescence intensity and lifetime changes or spectral shifts related to microenvironmental changes around the fluorophore. Environment-sensitive changes in the fluorescence intensity and lifetime of Cy3 have been successfully applied to the observation of the dynamics of protein–nucleic acid interactions.[21,22] However, it is still often challenging to achieve sufficient time resolution in single-molecule dynamic analysis based on environment-sensitive fluorophores.

Fluorescent signals from a single fluorophore often blink, reflecting time-dependent fluctuations between bright (ON) and dark (OFF) states.[23–26] While background fluorescence is a common obstacle in single-molecule fluorescence microscopy, a single fluorescence molecule exhibiting a controlled unique blinking pattern can be readily read out even against a high-fluorescence background. Blinking can occur in response to various chemical reactions and is involved in super-resolution microscopy.[27–29] Recently, we focused on control of the blinking kinetics or patterns to reflect microenvironment changes around the fluorophore. The kinetics of a reaction concomitant with blinking can be measured from the duration of the ON state (τ_{ON}) and that of the OFF state (τ_{OFF}) with a microsecond time resolution using fluorescence correlation spectroscopy (FCS). We developed a method we termed kinetic analysis based on the control of fluorescence blinking (KACB). In KACB, the nature of the OFF state plays the key role. The OFF state should form reversibly and should persist longer than one microsecond. KACB based on the formation of the following OFF states has been reported: a) a triplet state resulting from intersystem crossing,[30] b) a reduced state triggered by photoinduced electron transfer,[31–33] c) an isomerized state formed by *trans*-to-*cis* photoisomerization.[34] Since these OFF states are triggered by photoirradiation and hence the τ_{ON} value varies depending on the power intensity of the irradiation laser or the excitation efficiency, microenvironmental changes around the fluorophore are monitored by the τ_{OFF}. KACB allowed us to discriminate between DNA conformations around a fluoro-

[*] Prof. Dr. K. Kawai
The Institute of Scientific and Industrial Research (SANKEN)
Osaka University, Mihogaoka 8-1, Ibaraki, Osaka 567-0047 (Japan)
E-mail: kiyohiko@sanken.osaka-u.ac.jp
T. Miyata, Dr. N. Shimada, Prof. Dr. A. Maruyama
Department of Life Science and Technology
Tokyo Institute of Technology, 4259 B-57 Nagatsuta
Midori-ku, Yokohama, Kanagawa 226-8501 (Japan)
E-mail: amaruyama@bio.titech.ac.jp
Prof. Dr. S. Ito, Prof. Dr. H. Miyasaka
Division of Frontier Materials Science and
Center for Promotion of Advanced Interdisciplinary Research
Graduate School of Engineering Science, Osaka University
Toyonaka, 567-8531 226-8501 (Japan)
Supporting information and the ORCID identification number(s) for the author(s) of this article can be found under: https://doi.org/10.1002/anie.201708705.

phore, such as hairpin loops, duplexes, bulged duplexes, and triplexes. However, these measurements were performed under ensemble conditions, and the KACB has not been proven to be applicable to single-molecule detection and analysis. Herein, we show that redox-blinking-based KACB (rKACB) can be utilized for real-time single-molecule monitoring of the structural switching dynamics of nucleic acids between a hairpin loop and a stem structure.

We selected ATTO 655 as a fluorophore since it possesses high photostability and is frequently used in single- molecule fluorescence measurements.[35–39] The reduction potential of ATTO 655 is more positive than that of molecular oxygen (O_2),[39] and its reduced form (ATTO 655$^{\bullet-}$) reacts very slowly with O_2 (ca. s^{-1}).[36] Thus, by using ATTO 655, rKACB can be applied under aerobic conditions with no need for an enzymatic oxygen-scavenging system. Redox blinking can be triggered by adding a reductant and an oxidant to the solution. Tinnefeld and co- workers utilized redox reactions to increase the photostability of fluorophores by depopulating the triplet excited state.[36,37] In rKACB, we controlled redox blinking by using an ascorbic acid 2-phosphate (VcP) and iron(III) diethylenetriaminepentaacetic acid (FeDTPA) reductant/oxidant pair. During the repetitive cycle of excitation and emission, photoexcited ATTO 655 occasionally reacts with VcP to form the radical anion OFF state (ATTO 655$^{\bullet-}$). ATTO 655$^{\bullet-}$ then reacts with FeDTPA to regenerate intact ATTO 655, thereby returning the system to the ON state (Figure 1). rKACB relies on the accessibility of the fluorophore to the oxidant.[31] The more a fluorophore is exposed to a solvent, the faster the bimolecular collision reaction occurs, resulting in a decrease in the τ_{OFF} (Figure 2 a). Since DNA has two grooves that are widely opened to the solvent, a small oxidant such as O_2 can easily access the fluorophore even when it is intercalated with DNA. The key element of rKACB is refinement of the molecular shape and size of the oxidant; here we selected the bulky oxidant FeDTPA to make the τ_{OFF} more sensitive to microenvironmental changes at nucleic acids. While common reductant ascorbic acids

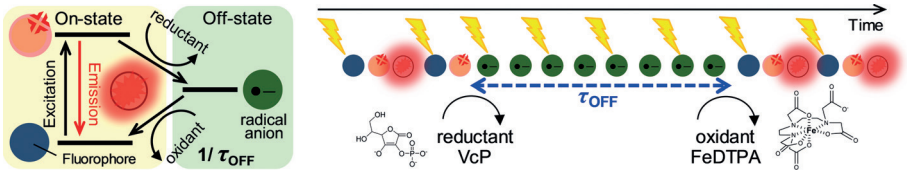

Figure 1. Schematic representation of the rKACB method. During the ON state, the fluorophore undergoes repetitive excitation and emission cycles. It enters the OFF state through the reaction with a reductant in the excited state to form the radical anion. The reaction of the radical anion OFF state with an oxidant regenerates the intact fluorophore to regenerate the ON state.

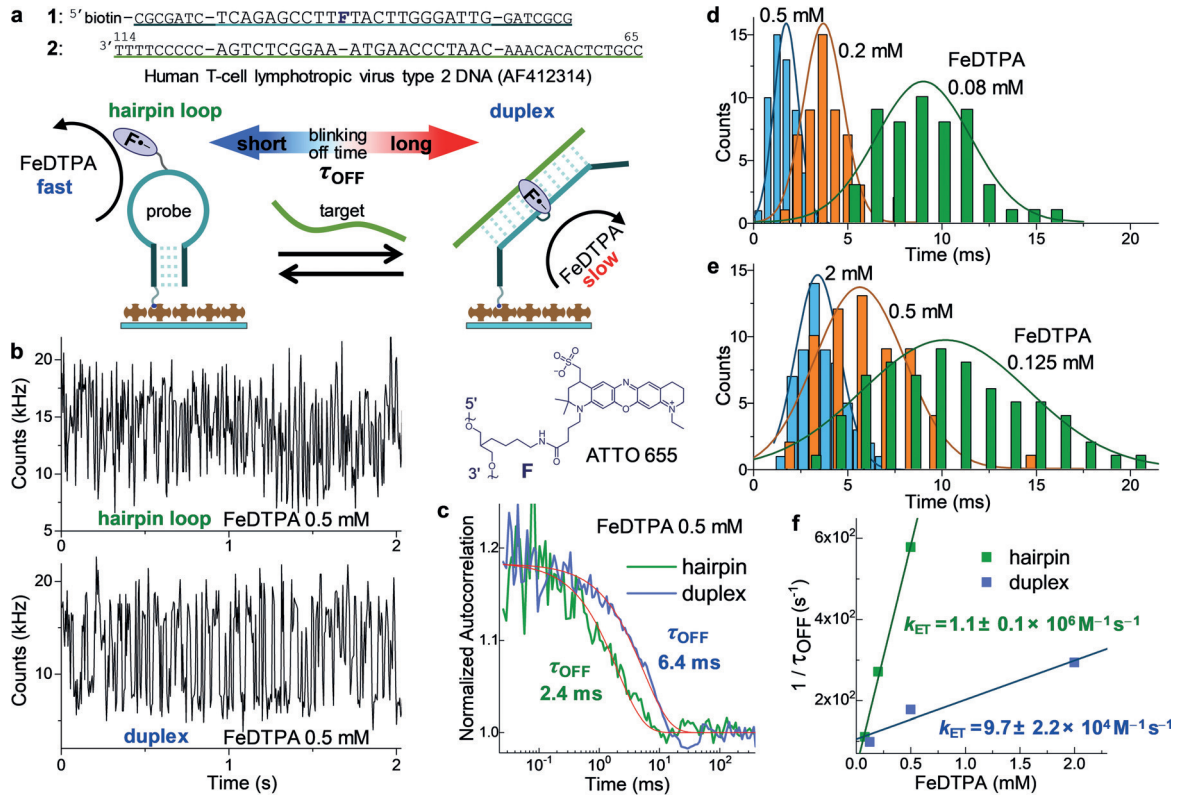

Figure 2. Discrimination between a hairpin and a duplex structure by rKACB. a) Design of molecular-beacon-type probe **1**. b) Representative fluorescence time trace obtained from a single **1** (hairpin loop) and **1:2** (duplex) molecule attached to the glass surface in the presence of 100 mM VcP and 0.5 mM FeDTPA. c) Autocorrelation analysis of fluorescence time traces in (b). d, e) Histograms of τ_{OFF} values measured from more than 50 individual ATTO 655 modified DNA molecules for each indicated FeDTPA concentration for hairpin loop **1** (d) and duplex **1:2** (e). f) Stern–Volmer plots for the electron-transfer reaction between ATTO 655$^{\bullet-}$ and FeDTPA.

reacted directly with FeDTPA and thus could not be used, the slightly weaker reductant VcP[40] served as a nice redox pair with FeDTPA.

rKACB was first tested for discrimination between a hairpin loop and a duplex conformation of DNA. ATTO 655 was attached at the loop region of the molecular-beacon-type probe **1** to expose it to the solvent. In the presence of the target gene human T-cell lymphotropic virus type 2 DNA [AF412314] (**2**),[41] ATTO 655 was buried in the context of the duplex (**1**:**2**) (Figure 2a). The molecular-beacon-type probe was tethered with biotin at the 5′-end and was immobilized on a glass surface through well-established streptavidin–biotin chemistry.

By utilizing confocal microscopy, the fluorophore was searched and fluorescence intensity fluctuation was measured by using an avalanche photodiode (APD).[42] Typical time-dependent fluorescence fluctuation signals for **1** and **1**:**2**, each recorded under 100 mM VcP and 0.5 mM FeDTPA, are shown in Figure 2b. Two-state ON and OFF blinking and one-step bleaching was observed, thus indicating that signals were obtained from a single ATTO 655 (see Figure S1 in the Supporting Information). The difference in blinking patterns between the two DNA structures is clearly distinguishable at a glance. Fast blinking was observed for ATTO 655 at the hairpin loop region, while ATTO 655 in the context of a duplex, where it is buried, showed slow blinking kinetics (Figure 2b; see Movie S1). rKACB was measured under various concentrations of FeDTPA, and a τ_{OFF} corresponding to the lifetime of ATTO 655$^{\bullet-}$ was obtained through auto-correlation analysis using the following Equation (1)[43–45] (Figure 2c).

$$G(\tau) = 1 + \left(\frac{\tau_{OFF}}{\tau_{ON}}\right) \exp\left(-\tau\left(\frac{1}{\tau_{OFF}} + \frac{1}{\tau_{ON}}\right)\right) \quad (1)$$

Figure 2d,e shows histograms of the τ_{OFF} measured from more than 50 individual ATTO 655-modified DNA molecules for each FeDTPA concentration. The τ_{OFF} was determined from the Gaussian fit. The τ_{OFF} decreased with an increase in the concentration of FeDTPA due to an increase in the collision probability. Thus the blinking pattern can be tuned by varying the concentration of the oxidant (see Figure S2). The bimolecular electron-transfer rate constant k_{ET} between ATTO 655$^{\bullet-}$ and FeDTPA was determined through Stern–Volmer analysis. By plotting $1/\tau_{OFF}$ against the concentration of FeDTPA, a linear relationship was obtained (Figure 2f), and k_{ET} was determined from the slope of the linear plot according to Equation (2),[31]

$$\frac{1}{\tau_{OFF}} = \frac{1}{\tau_0} + k_{ET}[\text{FeDTPA}] \quad (2)$$

where τ_0 is the τ_{OFF} in the absence of FeDTPA. As designed, the k_{ET} obtained for ATTO 655 was 11-fold larger when positioned at the hairpin loop region than when buried in the context of a duplex. This allows the monitoring of conformational changes between hairpin and a duplex structure at the single-molecule level. The reaction rate of a short-lived and usually non-emissive radical ion was conventionally determined through a transient absorption measurement. It is noteworthy that the bimolecular electron-transfer rate constant obtained herein was determined from fewer than 200 molecules, which is at least 10^{12} times fewer than the quantity typically required for transient absorption measurements (>1 nmol). The difference in the k_{ET} values obtained for hairpin loop and duplex structures was larger than that obtained when R6G was used as a fluorophore (3.7-fold difference).[31] This difference between R6G and ATTO 655 may stem from incomplete stacking of rhodamine dyes in the context of a duplex structures, as suggested in previous studies.[33,46] This is in line with our previous report that the nature of the fluorophore used is critically important for sensitive read-out of the microenvironment around the fluorophore in rKACB.[31]

To investigate whether rKACB is effective at monitoring the conformational switching dynamics of nucleic acids, we performed real-time single-molecule analysis of conformational switching of the preQ$_1$ riboswitch from *Fusobacterium nucleatum* mRNA.[47,48] This is the smallest known riboswitch, and its folding process has attracted attention as a model system to understand riboswitch folding.[49] Its aptamer domain specifically recognizes 7-aminomethyl-7-deazaguanine (preQ$_1$) and controls gene expression through ligand-mediated conformational switching. Using NMR spectroscopy, Micura and co-workers demonstrated that the riboswitch adopts two different coexisting stem-loop structures, fold **A** and fold **B** (Figure 3a).[48] The equilibrium of this bistable stem-loop segment were shown to shift to the fold **B** structure in the presence of preQ$_1$. We introduced ATTO 655 between positions A46 and A47 so as to bury ATTO 655 in the stem in the fold **A** structure while leaving it exposed to the solvent in the fold **B** structure.

rKACB was performed with 0.2 mM FeDTPA for preQ$_1$ riboswitch RNA attached to a glass surface for 20 molecules in the absence and 20 in the presence of 1 μM preQ$_1$, with total observation times of 956 sec and 752 sec, respectively. The fluctuation between the slow blinking pattern corresponding to ATTO 655 at the stem (fold **A**) and the fast blinking pattern corresponding to that at the loop (fold **B**) was analyzed (Figure 3b, Figure S3). Histograms of τ_{OFF} values are shown in Figure 3c. The two distributions, corresponding to slow blinking (stem) and fast blinking (loop), show that structural changes can be analyzed by a two-state model. Figure 3d shows histograms of the duration of the stem structure (τ_{Stem}) and loop structure (τ_{Loop}) that each followed a single-exponential distribution. The kinetics of the structural changes from fold **A** to fold **B** ($k_{A\rightarrow B}$), and from fold **B** to fold **A** ($k_{B\rightarrow A}$), were determined from the single-exponential fit of the distributions of τ_{Stem} and τ_{Loop}, respectively. The revealed kinetics of conformational switching between fold **A** and fold **B** structures were in the same order as for the preQ$_1$ induced structural switching rate obtained from stopped-flow measurements.[48] The addition of 1 μM preQ$_1$ resulted in an increase in $k_{A\rightarrow B}$, while $k_{B\rightarrow A}$ was almost unaffected. The equilibrium constant obtained from these rate constants ($K = k_{A\rightarrow B}/k_{B\rightarrow A}$) demonstrates that K shifts further toward fold **B** in the presence of 1 μM preQ$_1$, which is in line with the report by Micura and co-workers.[48] These results clearly demon-

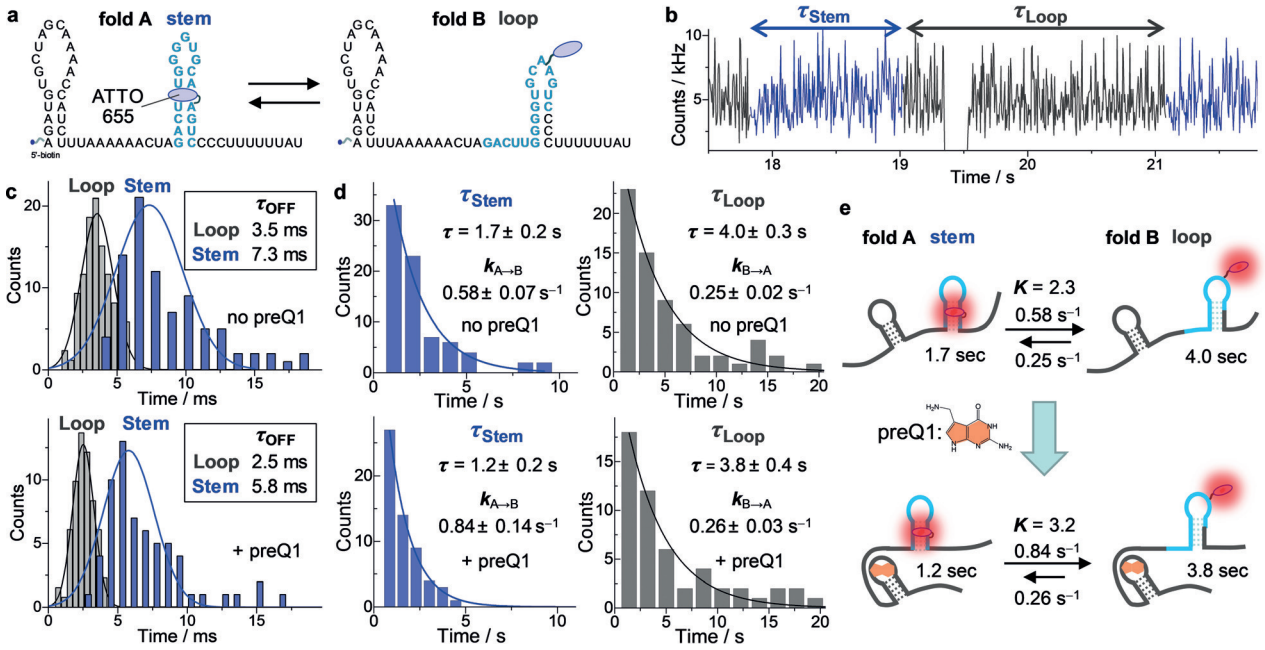

Figure 3. Real-time single-molecule analysis of the structural switching dynamics of preQ$_1$ riboswitch. a) A bistable secondary structure model for the riboswitch and the attachment site for ATTO 655. Twenty surface-immobilized molecules in the absence of preQ$_1$ and 20 in the presence of 1 μM preQ$_1$ were investigated. b) Representative fluorescence time trace obtained for the riboswitch attached to a glass surface. The τ_{OFF} value was measured for each appearance of stem (fold **A**) and loop (fold **B**) structures, and the durations of the structures, that is, τ_{Stem} and τ_{Loop}, were also obtained. c) Histograms of the appearance of stem and loop structures in the absence (above) and presence (below) of 1 μM preQ$_1$. d) Histograms of τ_{Stem} (left) and τ_{Loop} (right) in the absence (above) and presence (below) of 1 μM preQ$_1$. e) A schematic representation of the structural switching dynamics of the riboswitch, and the determined rate and equilibrium constants.

strate that the kinetics of structural changes of nucleic acids can be studied by rKACB at the single-molecule level.

In summary, we have demonstrated the rKACB method, which enables single-molecule real-time analysis of structural switching dynamics of nucleic acids between stem and loop structures. Subtle conformational changes in nucleic acids cannot be accessed by the conventional smFRET, and thus rKACB revealed unique dynamic information on nucleic acids. rKACB relies on blinking pattern changes that reflect the accessibility of a fluorophore to the oxidant. It can be applied to various systems by properly choosing the labeling site of a fluorophore so that its accessibility to the oxidant can be changed according to the structural or interaction dynamics of interest. The kinetics of blinking would be further tuned for each system by changing the shape and size of the oxidant and also by changing the concentration of the oxidant. rKACB, which requires labeling with only a single fluorophore and is easy to implement and provides a general and powerful tool for studying the structural and interaction dynamics of biomolecules.

Acknowledgements

Parts of this work were supported by JST PRESTO and the Center of Innovation (COI) Program; and by MEXT/JSPS KAKENHI Grant (16H01429 "Resonance Bio", 17H03088, 15K12755, 15H01807, JP26107002 "Photosynergetics", JP15H01096 "Nano-Material Optical-Manipulation" 16H03827).

Conflict of interest

The authors declare no conflict of interest.

Keywords: fluorescence · nucleic acids · RNA structures · sensors · single-molecule studies

How to cite: *Angew. Chem. Int. Ed.* **2017**, *56*, 15329–15333
Angew. Chem. **2017**, *129*, 15531–15535

[1] B. Schuler, E. A. Lipman, W. A. Eaton, *Nature* **2002**, *419*, 743–747.
[2] W. E. Moerner, D. P. Fromm, *Rev. Sci. Instrum.* **2003**, *74*, 3597–3619.
[3] E. M. S. Stennett, M. A. Ciuba, M. Levitus, *Chem. Soc. Rev.* **2014**, *43*, 1057–1075.
[4] S.-N. Uno, K. Tiwari Dhermendra, Y. Arai, T. Nagai, M. Kamiya, Y. Urano, *Microscopy* **2015**, *64*, 263–277.
[5] M. Levitus, S. Ranjit, *Q. Rev. Biophys.* **2011**, *44*, 123–151.
[6] T. Funatsu, Y. Harada, M. Tokunaga, K. Saito, T. Yanagida, *Nature* **1995**, *374*, 555–559.
[7] H. Noji, R. Yasuda, M. Yoshida, K. Kinosita, Jr., *Nature* **1997**, *386*, 299–302.
[8] S. Weiss, *Nat. Struct. Biol.* **2000**, *7*, 724–729.
[9] H. Yang, G. Luo, P. Karnchanaphanurach, T.-M. Louie, I. Rech, S. Cova, L. Xun, X. S. Xie, *Science* **2003**, *302*, 262–266.

[10] X. Michalet, S. Weiss, M. Jaeger, *Chem. Rev.* **2006**, *106*, 1785 – 1813.
[11] T. Ha, T. Enderle, D. F. Ogletree, D. S. Chemla, P. R. Selvin, S. Weiss, *Proc. Natl. Acad. Sci. USA* **1996**, *93*, 6264 – 6268.
[12] J. Hofkens, M. Cotlet, T. Vosch, P. Tinnefeld, K. D. Weston, C. Ego, A. Grimsdale, K. Muellen, D. Beljonne, J. L. Bredas, S. Jordens, G. Schweitzer, M. Sauer, F. De Schryver, *Proc. Natl. Acad. Sci. USA* **2003**, *100*, 13146 – 13151.
[13] R. Roy, S. Hohng, T. Ha, *Nat. Methods* **2008**, *5*, 507 – 516.
[14] T. Otosu, K. Ishii, T. Tahara, *Nat. Commun.* **2015**, *6*, 7685.
[15] M. S. T. Gonçalves, *Chem. Rev.* **2009**, *109*, 190 – 212.
[16] H. Kobayashi, M. Ogawa, R. Alford, P. L. Choyke, Y. Urano, *Chem. Rev.* **2010**, *110*, 2620 – 2640.
[17] A. Okamoto, *Chem. Soc. Rev.* **2011**, *40*, 5815 – 5828.
[18] A. S. Klymchenko, *Acc. Chem. Res.* **2017**, *50*, 366 – 375.
[19] M. K. Kuimova, S. W. Botchway, A. W. Parker, M. Balaz, H. A. Collins, H. L. Anderson, K. Suhling, P. R. Ogilby, *Nat. Chem.* **2009**, *1*, 69 – 73.
[20] B. E. Cohen, T. B. McAnaney, E. S. Park, Y. N. Jan, S. G. Boxer, L. Y. Jan, *Science* **2002**, *296*, 1700 – 1703.
[21] S. Myong, S. Cui, P. V. Cornish, A. Kirchhofer, M. U. Gack, J. U. Jung, K.-P. Hopfner, T. Ha, *Science* **2009**, *323*, 1070 – 1074.
[22] H. Hwang, H. Kim, S. Myong, *Proc. Natl. Acad. Sci. USA* **2011**, *108*, 7414 – 7418.
[23] E. K. L. Yeow, S. M. Melnikov, T. D. M. Bell, F. C. De Schryver, J. Hofkens, *J. Phys. Chem. A* **2006**, *110*, 1726 – 1734.
[24] S. van de Linde, M. Sauer, *Chem. Soc. Rev.* **2014**, *43*, 1076 – 1087.
[25] W. Zhang, M. Caldarola, B. Pradhan, M. Orrit, *Angew. Chem. Int. Ed.* **2017**, *56*, 3566 – 3569; *Angew. Chem.* **2017**, *129*, 3620 – 3623.
[26] Y. Zhang, P. Song, Q. Fu, M. Ruan, W. Xu, *Nat. Commun.* **2014**, *5*, 4238.
[27] R. Wombacher, M. Heidbreder, S. van de Linde, M. P. Sheetz, M. Heilemann, V. W. Cornish, M. Sauer, *Nat. Methods* **2010**, *7*, 717 – 719.
[28] S.-n. Uno, M. Kamiya, T. Yoshihara, K. Sugawara, K. Okabe, M. C. Tarhan, H. Fujita, T. Funatsu, Y. Okada, S. Tobita, Y. Urano, *Nat. Chem.* **2014**, *6*, 681 – 689.
[29] J. Vogelsang, C. Steinhauer, C. Forthmann, I. H. Stein, B. Person-Skegro, T. Cordes, P. Tinnefeld, *ChemPhysChem* **2010**, *11*, 2475 – 2490.
[30] K. Kawai, T. Koshimo, A. Maruyama, T. Majima, *Chem. Commun.* **2014**, *50*, 10478 – 10481.
[31] K. Kawai, K. Higashiguchi, A. Maruyama, T. Majima, *ChemPhysChem* **2015**, *16*, 3590 – 3594.
[32] K. Kawai, T. Majima, A. Maruyama, *ChemBioChem* **2013**, *14*, 1430 – 1433.
[33] K. Kawai, E. Matsutani, A. Maruyama, T. Majima, *J. Am. Chem. Soc.* **2011**, *133*, 15568 – 15577.
[34] K. Kawai, A. Maruyama, *Chem. Commun.* **2015**, *51*, 4861 – 4864.
[35] C. Eggeling, J. Widengren, L. Brand, J. Schaffer, S. Felekyan, C. A. M. Seidel, *J. Phys. Chem. A* **2006**, *110*, 2979 – 2995.
[36] J. Vogelsang, T. Cordes, C. Forthmann, C. Steinhauer, P. Tinnefeld, *Proc. Natl. Acad. Sci. USA* **2009**, *106*, 8107 – 8112.
[37] J. Vogelsang, T. Cordes, P. Tinnefeld, *Photochem. Photobiol. Sci.* **2009**, *8*, 486 – 496.
[38] S. Uphoff, S. J. Holden, L. Le Reste, J. Periz, S. van de Linde, M. Heilemann, A. N. Kapanidis, *Nat. Methods* **2010**, *7*, 831 – 836.
[39] Q. Zheng, S. Jockusch, G. G. Rodriguez-Calero, Z. Zhou, H. Zhao, R. B. Altman, H. D. Abruna, S. C. Blanchard, *Photochem. Photobiol. Sci.* **2016**, *15*, 196 – 203.
[40] T. Kuwahara, T. Homma, M. Kondo, M. Shimomura, *Biosens. Bioelectron.* **2011**, *26*, 3382 – 3385.
[41] M. C. Magri, L. F. d. M. Brigido, H. K. Morimoto, A. Caterino-de-Araujo, *AIDS Res. Hum. Retroviruses* **2013**, *29*, 1010 – 1018.
[42] H. Yamauchi, S. Ito, K.-i. Yoshida, T. Itoh, Y. Tsuboi, N. Kitamura, H. Miyasaka, *J. Phys. Chem. C* **2013**, *117*, 8388 – 8396.
[43] G. Bonnet, O. Krichevsky, A. Libchaber, *Proc. Natl. Acad. Sci. USA* **1998**, *95*, 8602 – 8606.
[44] W. Al-Soufi, B. Reija, M. Novo, S. Felekyan, R. Kuehnemuth, C. A. M. Seidel, *J. Am. Chem. Soc.* **2005**, *127*, 8775 – 8784.
[45] T. Kaji, S. Ito, S. Iwai, H. Miyasaka, *J. Phys. Chem. B* **2009**, *113*, 13917 – 13925.
[46] H. Bi, Y. Yin, B. Pan, G. Li, X. S. Zhao, *J. Phys. Chem. Lett.* **2016**, *7*, 1865 – 1871.
[47] M. Frener, R. Micura, *J. Am. Chem. Soc.* **2016**, *138*, 3627 – 3630.
[48] U. Rieder, C. Kreutz, R. Micura, *Proc. Natl. Acad. Sci. USA* **2010**, *107*, 10804 – 10809.
[49] K. C. Suddala, J. Wang, Q. Hou, N. G. Walter, *J. Am. Chem. Soc.* **2015**, *137*, 14075 – 14083.

Manuscript received: August 25, 2017
Accepted manuscript online: October 9, 2017
Version of record online: October 24, 2017

